

tained are differentially saturated and do not represent the total amounts of metabolites present. However, these signals can be corrected by using the known spin-lattice relaxation times (T_1 's) of the phosphate compounds and the nutation angles used (13). We have determined these parameters previously (13) and calculated the correction factors for CrP ($T_1 = 4.4$ seconds) and the beta phosphate of ATP ($T_1 = 1.63$ seconds) to be 1.94 and 1.27, respectively. With these values the actual CrP to ATP ratio is 2.2, in good agreement with our previous data (11, 13).

15. The signal-to-noise (S/N) ratios of peaks in these spectra were calculated using Nicolet 1280 software. As a criterion for retaining a data set, the S/N of the beta phosphate of ATP had to exceed 10 to 1, with 15 Hz line broadening applied. Since the ATP beta phosphate peak, an unresolved triplet, is several times broader than 15 Hz, this can be considered as a lower limit of the S/N value. This S/N allows changes of <10% in the phosphate resonance intensities to be observed. The values of CrP/ATP were calculated by using the Nicolet NMRCAPO routine to simulate experimental spectra as seven Lorentzian lines (three for ATP, one for CrP, one for phosphodiester, and two for the unresolved peaks of P_i , monophosphoesters, and 2,3-DPG), whose posi-

tions, heights, and widths were varied to minimize the root-mean-square deviation between experimental and simulated spectra.

16. The CrP/ATP values at low versus high heart rates were compared for each of the four points in the cardiac cycle by use of a paired one-tailed t test. The results gave $P > 0.15$ ($n = 6$ dogs) for each of the four phases. Only experiments with more than a 2.2-fold increase in the rate-pressure product with increased pacing rate were used in this analysis.

17. J. S. Ingwall, *Am. J. Physiol.* **242**, H729 (1982); J. A. Bitl and J. S. Ingwall, *J. Biol. Chem.* **260**, 3512 (1985); H. Hochrein, H. J. Doering, *Pflugers Arch.* **271**, 54 (1960).

18. E. T. Fossel, H. E. Morgan, J. S. Ingwall, *Proc. Natl. Acad. Sci. U.S.A.* **77**, 3654 (1980).

19. J. Wikman-Coffelt, R. Sievers, R. J. Coffelt, W. W. Parmley, *Am. J. Physiol.* **245**, H354 (1983).

20. A. P. Koretsky *et al.*, *Proc. Natl. Acad. Sci. U.S.A.* **80**, 7491 (1983).

21. L. N. Katz and H. Feinberg, *Circ. Res.* **6**, 656 (1958).

22. E. Rhode, *Arch. Exp. Pathol. Pharmacol.* **68**, 406 (1912); C. L. Evans and Y. Matsuoka, *J. Physiol. (London)* **49**, 378 (1915); P. L. Wilkinson, J. V. Tyberg, J. R. Moyers, A. E. White, *Anesth. Analg.* **59**, 233 (1980); H. R. Weiss, *Adv. Exp. Med. Biol.*

37A, 553 (1973); G. J. Grover and H. R. Weiss, *Am. J. Physiol.* **249**, H249 (1985).

23. In previous studies of dog hearts (21, 22) under various conditions, including anesthesia regimes similar to that used in the present study, the relationship of oxygen consumption (moles per minute per gram) and the rate-pressure product (mmHg per minute) has been shown to be linear with a slope of 0.4 to 0.6. Therefore the 5,000 to 25,000 range in the rate-pressure product in these studies indicates that the oxygen consumption of the heart was changing two- to threefold with the pacing jump.

24. R. G. Hansford, *Rev. Physiol. Biochem. Pharmacol.* **102**, 1 (1985). NAD is nicotinamide adenine dinucleotide and NADH is the reduced form.

25. We thank K. Metz for help with the gated acquisition experiments, and I. Gorman, C. Manusco, J. Minnich, H. Hughes, and W. White for helpful advice and technical assistance. Financial support from the Pennsylvania Affiliate of the American Heart Association, PHS Biomedical Research Support grant SO7RR05860-15, the Whitaker Foundation, PHS grant R23CA3927, and the intramural National Heart, Lung, and Blood research program is gratefully acknowledged.

27 November 1985; accepted 21 March 1986

AIDS Retrovirus Induced Cytopathology: Giant Cell Formation and Involvement of CD4 Antigen

JEFFREY D. LIFSON, GREGORY R. REYES,* MICHAEL S. MCGRATH, BARRY S. STEIN, EDGAR G. ENGLEMAN

The formation of multinucleated giant cells with progression to cell death is a characteristic manifestation of the cytopathology induced by the AIDS retrovirus in infected T lymphoid cells. The mechanism of giant cell formation was studied in the CD4 (T4/Leu 3) positive T cell lines JM (Jurkat) and VB and in variants of these lines that are negative for cell surface CD4 antigen. By means of a two-color fluorescent labeling technique, multinucleated giant cells in infected cultures were shown to form through cell fusion. Antibody to CD4 specifically inhibited fusion, and uninfected CD4 negative cells, in contrast to uninfected CD4 positive cells, did not undergo fusion with infected cells, suggesting a direct role for the CD4 antigen in the process of syncytium formation. These results suggest that, in vivo, cell fusion involving the CD4 molecule may represent a mechanism whereby uninfected cells can be incorporated into AIDS virus infected syncytia. Because the giant cells die soon after they are formed, this process may contribute to the depletion of helper/inducer T cells characteristically observed in AIDS.

THE T LYMPHOTROPIC RETROVIRUS known variously as LAV, HTLV-III, and ARV has been etiologically associated with the acquired immune deficiency syndrome (AIDS) and a spectrum of related disorders (1). Serum antibodies to viral antigens are found in most patients with these conditions (1, 2), and the virus is readily isolated from these individuals (2). In patients infected with the virus, the helper/inducer T lymphocyte subset, which bears the CD4 (T4/Leu 3) cell surface antigen, is characteristically depleted (3). In vitro, the virus is tropic and cytopathic for T cells and transformed cell lines expressing CD4, and monoclonal antibodies to CD4 block the infectivity of the virus in vitro (1, 2, 4-6). Thus CD4 may function as a specific cellular receptor for the AIDS virus (6).

The mechanism through which the AIDS virus induces cytopathology in susceptible cells is not well understood. In vitro, infected cells characteristically form multinucleated giant cells that produce large amounts of virus and then die over a period of a few days (1, 2). Multinucleated giant cells and cells expressing viral antigens have also been observed in histologic sections from infected individuals (7). Such cells may result from fusion of infected cells, or from uncoupling of the normal mechanisms that synchronize nuclear replication and cell division. We now present evidence that the CD4 molecule is involved in the fusion of infected cells and that CD4⁺ cells do not need to be productively infected themselves to undergo fusion with an already infected cell.

To study the cytopathic effects of the

AIDS retrovirus, we used two CD4⁺ leukemic T cell lines, JM (Jurkat) and VB, that respond to AIDS virus infection in a manner which approximates infection in nontransformed human T helper/inducer cells. Infection of these lines resulted in a burst of virus production [assessed by measuring cell-free, particle-associated reverse transcriptase (RT) activity] that was accompanied by a pronounced cytopathic effect. Virus production then declined over a period of days to weeks, and RT activity ultimately ceased altogether. Cell surface expression of the CD4 antigen decreased after infection, so that by the time detectable virus production had ceased, all the viable cells were essentially CD4⁻ (Fig. 1). Surface expression of other antigens, including CD3, CD5, CD7, and nonpolymorphic HLA class I determinants did not vary significantly between the initial CD4⁺ population and the CD4⁻ postinfection outgrowth. The JM CD4⁻ outgrowth was completely refractory to infection with the virus. To determine whether the CD4⁻ outgrowth was persistently but nonproductively infected, we used Southern blot analysis to test for the presence of the AIDS virus genome. No viral gene sequences were detected when the HTLV-III

J. D. Lifson and E. G. Engleman, Department of Pathology, Stanford University Medical School, Stanford, CA 94305; Palo Alto VA Medical Center, Palo Alto, CA 94303; and Stanford Medical School Blood Center, Palo Alto, CA 94304.

G. R. Reyes, Cancer Biology Research Laboratory, Department of Radiology, Stanford University, Stanford, CA 94305.

M. S. McGrath, Division of AIDS/Oncology, San Francisco General Hospital and University of California at San Francisco, San Francisco, CA 94110.

B. S. Stein, Department of Pathology, Stanford University Medical School, Stanford, CA 94305, and Stanford Medical School Blood Center, Palo Alto, CA 94304.

*Present address: Gene Labs, Inc., San Carlos, CA 94070.

proviral DNA clone HXB2 (8) was used as a hybridization probe (Fig. 2, A and B). In parallel experiments, infected CD4⁺ VB cells also yielded a CD4⁻ virus negative outgrowth. Viral antigens were not detectable in these CD4⁻ cells by immunofluorescence

analysis with sera from patients positive for AIDS virus antibodies, and coculture with uninfected CD4⁺ JM or VB cells did not result in detectable RT activity or cytopathology.

To account for the loss of virus production and cell surface CD4 expression, we

considered the possibility that the original JM cell line we used was not clonal. If this were the case, the CD4⁻ outgrowth could have reflected overgrowth by a CD4⁻, non-JM contaminant of the predominant CD4⁺ JM cells. We therefore analyzed both the original JM cells and the CD4⁻ postinfection outgrowth by the Southern blot technique, using the YT-35 DNA clone for the T cell receptor (TCR) β -chain (9). Both the parental JM cell line and the CD4⁻ postinfection JM outgrowth displayed the TCR β -chain gene rearrangement pattern expected for the JM cell line (Fig. 2C) (9). These results suggested that the CD4⁻ outgrowth was not the result of contamination of the original cell line but arose as a consequence of selective pressure in the infected clonal cultures. Approximately 1% to 3% of cells were CD4⁻ at the time of infection; these CD4⁻ cells apparently resist AIDS virus infection and cytopathology, and are able to survive. Other investigators have reported CD4⁻, AIDS virus positive outgrowths of infected CD4⁺ cultures, suggesting that AIDS virus infection may lead to decreased expression of CD4 (10). Although our studies do not formally rule out the possibility of latent viral infection, below the threshold of the assays used, the absence of detectable virus suggests that our CD4⁻ cells were not generated through this mechanism.

We next used the JM and VB cell lines and their CD4⁻, virus negative postinfection outgrowths to examine the mechanism of giant cell formation and evaluate the role of the CD4 molecule in AIDS virus induced cytopathology. A two-color fluorescent labeling technique was used to identify cell populations in cell mixing experiments. Briefly, a population of CD4⁺ cells was infected with virus and cultured until giant cell formation began. The cells were then surface-labeled with rhodamine isothiocyanate (RITC) (11). A second population of uninfected cells, either CD4⁺ cells or a CD4⁻ outgrowth of the same cell line, was surface-labeled with fluorescein isothiocyanate (FITC) (11) and mixed in equal numbers with the RITC-labeled infected cells. The cells were cultured at 37°C in the presence and absence of a monoclonal antibody to CD4 or a control antibody and were evaluated by fluorescence microscopy at various time points after mixing. The fluorescent labeling procedure did not affect the viability or growth of the cells when compared to unlabeled parallel cultures.

One hundred multinucleated giant cells, defined as greater than four times the diameter of uninfected cells, were scored for each sample. These cells were evaluated for the presence of unequivocal red (RITC) or green (FITC) fluorescence by an observer

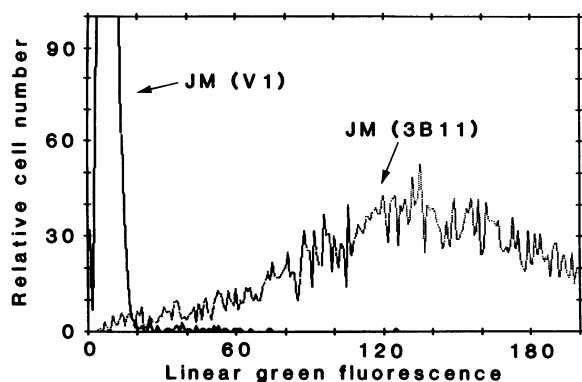


Fig. 1. Expression of cell surface CD4 on the parent JM cell line (JM3B11) and on postinfection outgrowth of JM cells (JMVI). Uninfected cells and the postinfection outgrowth were stained at 4°C with FITC-conjugated monoclonal antibody to CD4 at a saturating concentration of 2 μ g of antibody per 1.0×10^6 cells (13). Relative green fluorescence intensity is plotted against cell number for uninfected cells (dotted line) and postinfection outgrowth (solid line). Fluorescence of the postinfection outgrowth was indistinguishable from background.

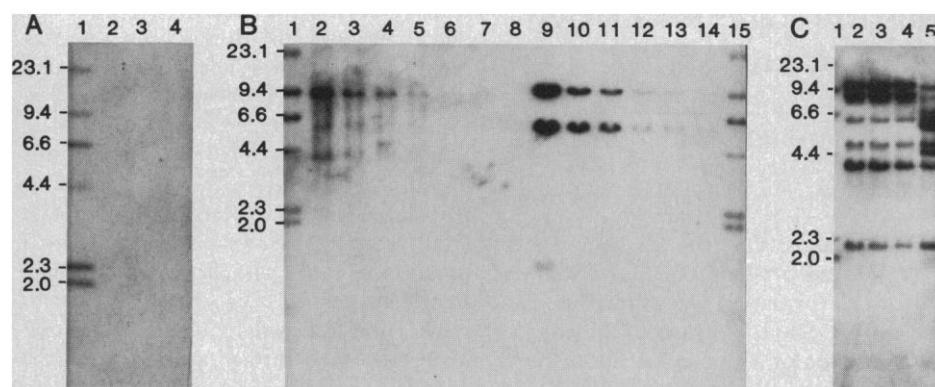


Fig. 2. The CD4⁻ postinfection JM outgrowth is virus negative and has the T cell receptor (TCR) β -chain gene pattern expected for the JM cell line. (A) The original JM cell line (lane 2) and two different CD4⁻ postinfection JM outgrowths (lanes 3 and 4) evaluated for the presence of AIDS virus DNA by Southern blot analysis of total cellular DNA after cleavage with Eco RI. Cleavage with this enzyme should release a specific internal viral fragment, irrespective of flanking host sequences, allowing detection of viral DNA. Eco RI-digested DNA (30 μ g per lane) was subjected to electrophoresis on a 0.8% horizontal agarose slab gel, transferred to nitrocellulose (14), and probed with HXB2 DNA (mixture of the two large internal Sac I fragments) (8) labeled with ³²P by nick translation to detect AIDS virus-specific sequences. No hybridization was seen. Lane 1 is phage λ DNA, used for size markers after cleavage with Hind III, dephosphorylation, and labeling with λ -³²P-ATP and polynucleotide kinase. (B) Copy number positive hybridization controls indicating sensitivity of the procedure. DNA from AIDS virus infected VB cells was mixed with total cellular DNA from noninfected VB cells (lanes 2 to 7). Mixed DNA was then cleaved with Eco RI and subjected to electrophoresis (7.5 μ g per lane), transferred to nitrocellulose (14), and probed with ³²P-labeled HXB2 DNA. Lanes 1 and 15, phage λ size markers. Relative amounts of infected VB cell DNA to total DNA in lanes 2 to 8 are: lane 2, all infected VB cell DNA; lane 3, 1:2; lane 4, 1:5; lane 5, 1:10; lane 6, 1:50; lane 7, 1:100; lane 8, all uninfected VB cell DNA. To determine the sensitivity of the hybridization procedure in terms of copies of AIDS virus genome detectable, HXB2 plasmid DNA was mixed with total cellular DNA from the uninfected B lymphoid cell line DHL1 (15) in proportions corresponding to the copy numbers specified below. Copy numbers for HXB2 plasmid DNA mixed with DHL1 DNA (lanes 9 to 14) are: lane 9, 5:1 (five full viral genome copies per one cell DNA equivalent); lane 10, 1:1; lane 11, 1:2; lane 12, 1:10; lane 13, 1:50; lane 14, 1:100. Detection of AIDS virus DNA from infected VB cells (approximately 50% viral antigen positive) mixed with uninfected VB DNA extends to approximately one infected cell per 50 cells total DNA equivalent. Hybridization to HXB2 plasmid DNA mixed with DHL1 DNA shows a sensitivity of approximately one copy of viral genome per 100 cells DNA equivalent. Results shown are for a 24-hour exposure of Kodak XAR-5 film, with intensifying screens; increased exposure time gave a slight improvement in sensitivity. (C) To assess TCR β -chain gene rearrangements, 7.5 μ g of total cellular DNA from JM cells (lane 2) and two distinct CD4⁻ derivatives (lanes 3 and 4) were cleaved with Eco RI, subjected to electrophoresis, transferred to nitrocellulose, and probed as above, using the YT-35 DNA clone (9) as a hybridization probe. Results show the hybridization pattern expected for JM cells, indicating the clonal identity of the CD4⁺ parent cells and the CD4⁻ derivatives. Comparison of the JM rearrangement pattern (lanes 2 to 4) with the germline configuration exhibited by the B cell lymphoma cell line DHL1 (lane 5) (15) reveals several differences. Size markers (lane 1) are as in (A) and (B).

Table 1. Giant cell formation involving CD4. Cells were labeled and scored as described in the text and Fig. 3. If no fusion between infected (red) cells and uninfected (green) cells occurred, red only giant cells would be expected, reflecting those present at the initiation of the culture and those formed during culture within the red labeled population. Giant cells scored red and green are indicative of fusion between cells of the two labeled populations. Giant cells were present in the culture treated with antibody to CD4 (20 $\mu\text{g}/\text{ml}$), at approximately one-tenth the frequency observed in untreated cultures or cultures treated with control antibodies (anti-CD3, anti-CD5, anti-CD7, anti-HLA class I), suggesting that antibody to CD4 inhibited fusion-mediated giant cell formation both between the two labeled populations and within the red labeled (infected) population.

Cell populations	Percentage of multinucleated giant cells at 48 hours	
	Red only	Red and green
Infected (CD4 ⁺) (red) plus uninfected (CD4 ⁺) (green)	16	84
Infected (CD4 ⁺) (red) plus uninfected (CD4 ⁻) (green)	95	5
Infected (CD4 ⁺) (red) plus uninfected (CD4 ⁺) (green) plus antibody to CD4	82	18

unaware of the identity of the samples being scored. Filters eliminated spectral overlap of the fluorochromes. Giant cells arising from the original RITC-labeled infected cell population would be expected to show only red fluorescence. Giant cells showing both red and green fluorescence would result from fusion of uninfected (green, FITC-labeled) cells with infected (red, RITC-labeled) cells. As shown in Table 1, uninfected (green)

CD4⁺ cells mixed with infected (red) cells showed a high percentage of giant cells with both red and green fluorescence (Fig. 3, a and b). When CD4⁻ uninfected (green) cells were mixed with infected (red) cells, virtually all the giant cells showed only red fluorescence (Fig. 3, c and d). Thus CD4⁻ cells did not undergo fusion with infected cells and there was not significant transfer of fluorochromes between the two labeled

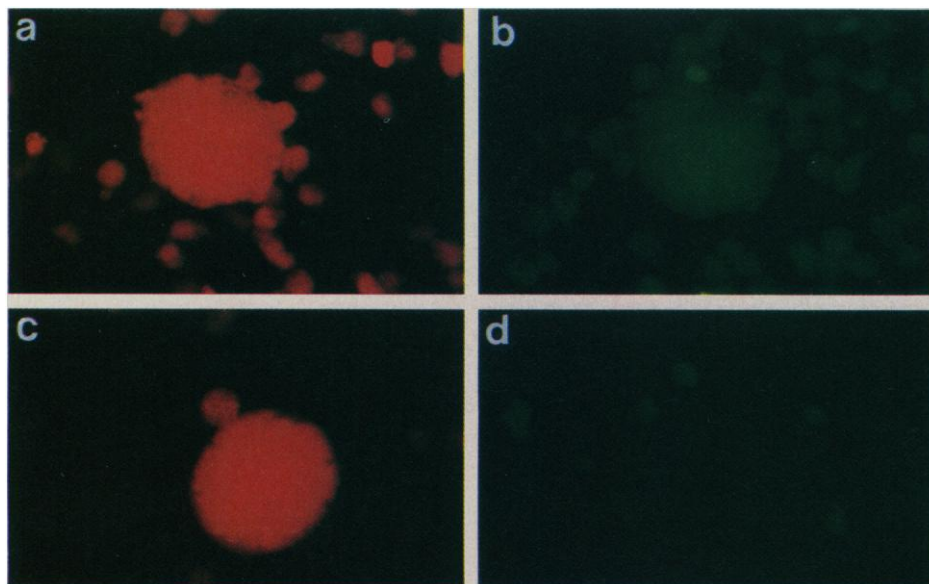


Fig. 3. Giant cell formation mediated by CD4-dependent cell fusion. Cells were surface-labeled with FITC and RITC as described (11, 16). Labeled cells were mixed in the indicated combinations at equal numbers, cultured at 37°C, then fixed in 0.37% formaldehyde with PBS (v/v), and scored on a Zeiss Universal photomicroscope equipped for epifluorescence. Results shown are for the VB cell line scored at 48 hours, when approximately 60% of the cells were involved in syncytia. Initial formation of two-color giant cells was noted as early as 3 hours after mixing of cells. The cells shown were from a culture in which infected (RITC-labeled) VB cells were mixed with uninfected (FITC-labeled) CD4⁺ VB cells (a and b) or with an uninfected (FITC-labeled) CD4⁻, virus negative outgrowth of a previously infected VB culture (c and d). The same field was photographed with filters to observe either red or green fluorescence. Note normal sized cells showing either only red or only green fluorescence. In contrast, the multinucleated giant cell in (a) and (b) (400 \times original magnification) demonstrates unequivocal fluorescence for both RITC (a) and FITC (b), indicative of cell fusion. The giant cell in C and D (400 \times) shows only red fluorescence. Similar results were obtained in parallel experiments with the JM cell line and its CD4⁻ outgrowth, and when H9 cells were used as the infected component of the assay system with uninfected VB or JM cells.



Fig. 4. Inhibition of protein synthesis by cycloheximide. Cycloheximide treatment (10 $\mu\text{g}/\text{ml}$) inhibited greater than 90% of [³⁵S]methionine incorporation into trichloroacetic acid precipitable protein by uninfected VB cells, AIDS virus infected H9 cells, and by mixed cultures. Inhibition of protein synthesis reached its maximum within 30 minutes of exposure to the drug. Metabolic labeling with [³⁵S]methionine followed by SDS-PAGE and autoradiography confirmed the absence of protein synthesis in the cycloheximide-treated cells (17); 8% SDS-PAGE shows total cellular protein. Lane 1, untreated, uninfected VB cells; lane 2, uninfected, cycloheximide-treated VB cells; lane 3, untreated, infected H9 cells; lane 4, cycloheximide-treated, infected H9 cells; lane 5, untreated, mixed uninfected VB and infected H9 cells; lane 6, cycloheximide-treated, mixed uninfected VB cells and infected H9 cells.

populations in the absence of fusion. When CD4⁺ uninfected (green) cells were mixed with infected (red) cells in the presence of monoclonal antibody to CD4, giant cells occurred at a greatly reduced frequency, and most of them were red only, reflecting those giant cells already present in the red labeled population at the time of mixing. Monoclonal antibodies to CD3, CD5, CD7, and nonpolymorphic HLA class I determinants, also expressed by the cells tested, did not interfere with the formation of mixed color giant cells. Thus, cell-to-cell fusion is the mechanism of giant cell formation in infected cultures and the CD4 molecule appears to participate in the process.

We next addressed the question of whether all cells involved in fusion leading to giant cell formation had to be productively infected for the process to occur. We used the fluorescent labeling technique described above in combination with indirect immunofluorescence analysis using a patient-derived immunoglobulin G (IgG) preparation. This preparation was demonstrated by immunoprecipitation to contain reactivity against the major structural proteins of the AIDS virus. Unlabeled AIDS virus infected cells and RITC surface-labeled uninfected cells were separately treated with cycloheximide, then mixed and cultured in the continued presence of the drug. After 4 hours the cells were fixed, then stained by indirect

immunofluorescence (FITC) to detect viral antigen expression. In the presence of cycloheximide, even if virus were to gain entry into an initially uninfected cell, synthesis of

viral antigens could not occur (Fig. 4). Nevertheless, as shown in Fig. 5, a to h, cycloheximide treatment did not interfere with the fusion process. Cycloheximide had

no effect on the formation of viral antigen (FITC)-positive giant cells, which also showed RITC fluorescence, indicative of fusion with uninfected surface-labeled cells. Thus, infection of a CD4⁺ cell, with resulting synthesis of viral proteins, is not required for such a cell to fuse to another already infected cell displaying viral antigens on its surface.

The exact mechanism of fusion remains to be elucidated, but presumably involves interactions between CD4 molecules on one susceptible target cell and antigens determined by AIDS virus infection, most likely the viral envelope glycoprotein (12), expressed on another cell. Because the giant cells die shortly after they are formed, cell fusion leading to cell death may be one of the mechanisms accounting for the progressive depletion of CD4⁺ T helper/inducer lymphocytes observed in patients infected with the AIDS virus.

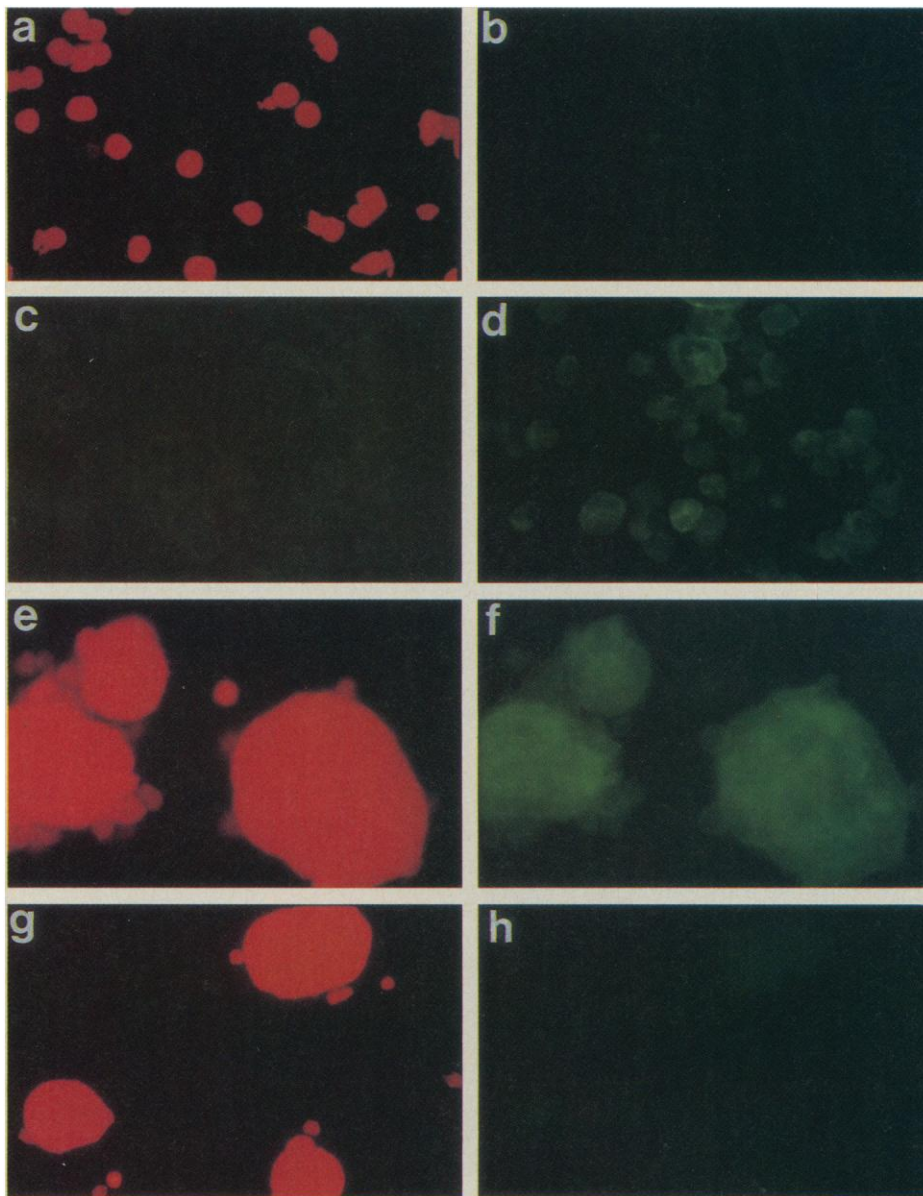


Fig. 5. Uninfected VB cells fuse with HTLV-III-infected H9 cells: Fusion is unattenuated by high dose cycloheximide. Uninfected VB cells (labeled with RITC as described for Fig. 3) and AIDS virus infected H9 cells (not labeled) were independently treated with 10 µg/ml of cycloheximide for 1 hour at 37°C to inhibit protein synthesis (see Fig. 4). The treated VB cells (RITC-labeled) were mixed with cycloheximide-treated, infected H9 cells (not RITC-labeled) in equal numbers (2×10^6) and incubated at 37°C for 4 hours with cycloheximide (19). The unmixed cell populations were incubated in a similar manner. After incubation the cells were fixed in gradient paraformaldehyde (2%, 4%, 8%) with subsequent staining by FITC-indirect immunofluorescence (20) for viral specific antigens using the IgG fraction (21) of serum from an AIDS virus seropositive patient. (a) RITC-positive uninfected VB cells (RITC-labeled) treated with cycloheximide for 4 hours; (b) Same field as (a) showing absence of FITC immunofluorescence for AIDS virus associated proteins. (c) Absence of FITC immunofluorescence for AIDS virus associated proteins in cycloheximide-treated, uninfected H9 cells (not RITC-labeled). (d) Positive FITC immunofluorescence for AIDS virus associated proteins in cycloheximide-treated, AIDS virus infected H9 cells (not RITC-labeled). (e) RITC-positive giant cells appearing 4 hours after mixing of cycloheximide-treated, uninfected VB cells (RITC-labeled) and cycloheximide-treated, AIDS virus infected H9 cells (not RITC-labeled). (f) Same field as (e) showing positive FITC immunofluorescence for AIDS virus associated proteins in giant cells. (g) RITC-positive giant cells appearing 4 hours after mixing of cycloheximide-treated, uninfected VB cells (RITC-labeled) and cycloheximide-treated, AIDS virus infected H9 cells (not RITC-labeled) and not subjected to FITC-indirect immunofluorescence for the virus-associated proteins. (h) Same field as (g) showing negligible background fluorescence during FITC excitation compared to (f). Original magnification: (a to f) 400×; (g and h) 250×.

REFERENCES AND NOTES

1. F. Barré-Sinoussi *et al.*, *Science* **220**, 868 (1983); M. Popovic, M. G. Sarngadharan, E. Read, R. C. Gallo, *ibid.* **224**, 497 (1984); J. A. Levy *et al.*, *ibid.* **225**, 840 (1984).
2. M. G. Sarngadharan, M. Popovic, L. Bruch, J. Schüpbach, R. C. Gallo, *ibid.* **224**, 506 (1984); F. Brun-Vezinet *et al.*, *Lancet* **1984-II**, 1253 (1984); R. C. Gallo *et al.*, *Science* **224**, 500 (1984).
3. J. L. Fahey *et al.*, *Am. J. Med.* **76**, 95 (1984).
4. D. Klatzmann *et al.*, *Science* **225**, 59 (1984).
5. M. Popovic, E. Read-Connole, R. C. Gallo, *Lancet* **1984-II**, 1472 (1984); J. D. Lifson and E. G. Engleman, unpublished observations.
6. A. Dalglish *et al.*, *Nature (London)* **312**, 763 (1984); D. Klatzmann *et al.*, *ibid.*, p. 767.
7. D. Pekovic, paper presented at the International Conference on AIDS, Atlanta, GA, 15 to 17 April 1985; L. R. Sharer, C. Eun-Sook, L. G. Epstein, *Hum. Pathol.* **16**, 760 (1985).
8. A. G. Fisher *et al.*, *Nature (London)* **316**, 262 (1985).
9. Y. Yanagi *et al.*, *ibid.* **308**, 145 (1984); F. Flug, P. Pelicci, F. Bonetti, D. M. Knowles, R. Dalla-Favera, *Proc. Natl. Acad. Sci. U.S.A.* **82**, 3460 (1985).
10. J. A. Hoxie *et al.*, *Science* **229**, 1400 (1985); T. Folks *et al.*, *ibid.* **231**, 600 (1986).
11. E. C. Butcher and I. L. Weissman, *J. Immunol. Methods* **37**, 97 (1980).
12. J. S. Allan *et al.*, *Science* **228**, 1091 (1985); R. C. Nowinski *et al.*, *Virology* **111**, 84 (1981); A. Pinter *et al.*, *J. Virol.* **57**, 1048 (1986); J. D. Lifson *et al.*, in preparation.
13. JM cells were infected by incubation with LAV-containing culture supernatant at 37°C for 1 hour (the RT activity was 5000 cpm per 1.0×10^6 cells). Cells were then cultured and showed characteristic cytopathology and a peak of virus production from days 5 through 10. RT activity then declined, and after 4 weeks was no longer detectable in cell-free culture supernatants. For all of these studies we used the monoclonal antibody to CD4 that is designated S3.5 (murine IgG_{2a}) and is produced in our laboratory. Sequential immunofluorescence binding studies suggest that the determinant on CD4 identified by S3.5 is near the Leu 3a epitope, but distinct from the OKT4 epitope. CD4⁻ cells were also negative for cell surface immunofluorescence when tested with antibody to Leu 3a and OKT4.
14. E. Southern, *J. Mol. Biol.* **98**, 503 (1975).
15. A. L. Epstein *et al.*, *Cancer* **42**, 2379 (1978).
16. Cells in the log phase of growth were washed in phosphate-buffered saline (PBS), then resuspended at 10^7 cells per milliliter in PBS containing either 50 µg/ml of FITC or 3 µg/ml of RITC (BBL, Cockeysville, MD). After incubation for 20 minutes at 37°C (FITC) or 25°C (RITC), RPMI 1640 culture medium containing 10% fetal calf serum (FCS) was added to absorb fluorochrome not bound to cell

surface proteins. Labeled cells were washed in PBS, then resuspended in RPMI 1640 medium containing 10% FCS at 10^6 cells per milliliter for culture.

17. Approximately 1×10^7 cells were washed in PBS and metabolically labeled with 150 μ Ci of [35 S]methionine for 4 hours in 5 ml of methionine-free RPMI 1640 medium containing 10% dialyzed FCS \pm 10 μ g/ml of cycloheximide. Cells labeled in the presence of cycloheximide were treated for 1 hour before the addition of the radioisotope. After 4 hours of incubation the cells were washed extensively in ice-cold PBS and solubilized in 0.5 ml of 2% Triton X-100 in PBS, pH 7.4. Insoluble material was then pelleted by centrifugation at 10,000g for 10 minutes. Portions (100 μ l) of cell extract were then mixed with 100 μ l of 2 \times electrophoresis buffer [6% sodium dodecyl sulfate (SDS), 10% glycerol, 0.125M tris-HCl, pH 6.8, and 5% β -mercaptoethanol] and boiled for 2 minutes. The extract was then run on a standard gel [8% SDS-polyacrylam-

ide gel electrophoresis (PAGE)] according to the method of Laemmli (18). The gel was fixed, impregnated with ENLIGHTENING (New England Nuclear) and exposed to Kodak X-Omat AR film with intensifying screens; optimal gel exposure was 7 hours. Trichloroacetic acid precipitable counts were determined from remaining cell extract not used for SDS-PAGE.

18. V. K. Laemmli, *Nature (London)* **227**, 680 (1970).
19. Uninfected VB cells and HTLV-III/LAV-infected H9 cells were chosen for this experiment because with this combination of cells, extensive fusion occurs within 4 hours. High doses of cycloheximide could thus be used to inhibit protein synthesis without compromising cell viability during the course of the experiment. The findings described in cycloheximide-treated cells were essentially identical to those for untreated cells both qualitatively and quantitatively, as well as temporally.
20. B. S. Stein *et al.*, *J. Biol. Chem.* **259**, 14762 (1984).

21. R. A. Kekwick, *Biochem. J.* **34**, 1248 (1940).

22. We thank J. C. Chermann for providing the reference isolate of LAV, T. Mak for providing the YT-35 clone, F. Wong-Staal, A. Fisher, and R. Gallo for providing the H9 cells and HXB2 provirus clone, S. Smith for the VB cell line, M. Feinberg for discussions, C. Benike for review of the manuscript, R. Coffin and P. Horne for photography, D. Sasaki for flow cytometry analysis, and D. Jones for secretarial assistance. J.D.L. and G.R.R. were postdoctoral fellows of the Damon Runyon-Walter Winchell Cancer Fund (DRG-021 and DRG-718, respectively); J.D.L. is the recipient of a Career Development Award from the Veterans Administration. Supported in part by NIH grant HL32453, the Medical Research Service of the Veterans Administration, and the California State AIDS Task Force.

12 December 1985; accepted 16 April 1986

Protein, DNA, and Virus Crystallography with a Focused Imaging Proportional Counter

R. M. DURBIN,* R. BURNS, J. MOULAI, P. METCALF, D. FREYMAN, M. BLUM, J. E. ANDERSON, S. C. HARRISON, D. C. WILEY

A set of programs has been developed for rapid collection of x-ray intensity data from protein and virus crystals with a commercially available two-dimensional focused geometry electronic detector. The detector is compact and portable, with unusually high spatial resolution comparable to that used in oscillation photography. It has allowed x-ray data collection on weakly diffracting crystals with large unit cells, as well as more conventional "diffractometer-quality" crystals. The quality of the data is compared with that from oscillation photography and automated diffractometry in the range of unit cells from 96.3 to 383.2 angstroms. Isomorphous and anomalous difference Pattersons, based on detector data, are shown for a variable surface glycoprotein mercury derivative and for a repressor-DNA bromine derivative, which has been solved at 7 angstroms with detector data only.

THE MOST EFFICIENT METHOD OF collecting x-ray diffraction data is to record at one time with a photon counting detector as many as possible of the simultaneously occurring x-ray reflections. Conventional proportional counters have no spatial resolution, and thus conventional diffractometers collect only one or a few reflections at once. Film is an efficient but imperfect area detector, and widely used in the unit cell range above 100 \AA (1). After the pioneering work by Xuong (2, 3) and by Arndt (4), several groups have developed data collection systems using two-dimensional photon counting electronic detectors with sufficient spatial resolution to assign every diffracted photon to the correct reflection (4, 5).

We have written software for rapid data collection with a novel commercially available detector that is portable enough to be moved from one x-ray generator to another in the laboratory. The detector generates a 512 by 512 pixel image of all simultaneously occurring diffraction. Its total angular subtense is 60 degrees when set at 11 cm from

the crystal. A 5 minutes of arc oscillation exposure of tomato bushy stunt virus (TBSV) (Fig. 1) demonstrates a novel feature of this instrument—high spatial resolution. The 512 by 512 pixel image has about 200- μ m resolution at the detector face. This makes it roughly equivalent to digital film scanning with a 200- μ m raster, except that the counter suffers none of the spot-edge effects (6) that limit optical density raster-scanning. Thus, the only condition to be met is that adjacent reflections be spatially resolved. Using Franks double mirror focusing optics (7) on an Elliot GX-6 rotating anode, unit cell dimensions in the 100 to 180 \AA range are readily resolved at crystal to detector distances of 10 cm, and larger cells are resolved at 18 cm. Figure 1 shows diffraction from crystals of TBSV ($a = 385 \text{\AA}$). The spots within the marked circle (Fig. 1A) at 2.6 \AA resolution (specimen to detector distance 18 cm) can be seen on an expanded scale (Fig. 1B) to form a resolved, centered lattice.

The x-ray detector is a focused geometry imaging proportional counter, which is part

of a data collection system (Nicolet-Xentronics, Madison, WI). The counter is a sealed, xenon-filled unit, with a concave Be window (11.5 cm in diameter). The curvature reduces parallax at the edges of the detector by making the electric field lines more parallel to the path of the incident photons in the interaction zone near the front window. The signal is collected on a multiwire anode and read capacitively on cathodes of more finely spaced wires (one set of wires in x and one in y). The detector and position-determining circuit combine a coarsely segmented cathode (2 cm) with capacitive charge division within a segment to produce resolution of 0.20-mm full width at half height. High resolution is achieved in both the x and y dimensions because electrons created in the initial ionization event are allowed to diffuse in the drift space, creating a relatively large (3 to 4 mm) cloud of ions. The distribution of the electrons is recorded on a number of wires from which the centroid (and therefore the photon position) can be calculated to a fraction of the actual wire spacing. The current instrument has six cathode segments in each direction and 12-bit analog to digital converters. The electronics have a dead time of 5 μ sec. The current limiting factor for data collection rate is the 18- μ sec time required by the data collection microcomputer to record and map (see below) each event. This characteristic permits acquisition rates up to 60 kHz at 50% dead-time loss (the unmapped mode rate is 100 kHz). Our experience indicates that the data rate is limited by the power available from our x-ray source (Elliot GX-6

R. M. Durbin, J. Moulai, P. Metcalf, D. Freyman, M. Blum, J. E. Anderson, S. C. Harrison, D. C. Wiley, Department of Biochemistry and Molecular Biology and Committee on Higher Degrees in Biophysics, Harvard University, 7 Divinity Avenue, Cambridge, MA 02138. R. Burns, Nicolet-Xentronics Corp., Verona Road, Madison, WI 53711.

*Present address: MRC Laboratory of Molecular Biology, Hills Road, Cambridge CB2 2QH, England.